Evaluating atmospheric electricity changes as an indicator of fog formation

Miller, C., Nicoll, K. A. ORCID: https://orcid.org/0000-0001-5580-6325, Westbrook, C. ORCID: https://orcid.org/0000-0002-2889-8815 and Harrison, R. G. ORCID: https://orcid.org/0000-0003-0693-347X (2024) Evaluating atmospheric electricity changes as an indicator of fog formation. Quarterly Journal of the Royal Meteorological Society, 150 (761). pp. 1892-1906. ISSN 1477-870X doi: https://doi.org/10.1002/qj.4680 Available at https://centaur.reading.ac.uk/114920/

Received: 29 September 2023 | Revised: 5 January 2024 | Accepted: 20 January 2024

DOI: 10.1002/qj.4680

Quarterly Journal of the Royal Meteorological Society RMetS

RESEARCH ARTICLE

Evaluating atmospheric electricity changes as an indicator of fog formation

Caleb Miller | **Keri A. Nicoll** | **Chris Westbrook** | **R. Giles Harrison**

Department of Meteorology, University of Reading, Reading, UK

Correspondence
Caleb Miller, Department of Meteorology, University of Reading, Reading, UK.
Email: c.s.miller@pgr.reading.ac.uk

Funding information
Natural Environment Research Council, Grant/Award Number: NE/S007261/1

Abstract

Fog is a high-impact weather phenomenon, which is challenging to forecast accurately. Measuring changes in atmospheric electricity has been proposed as a complement to other fog prediction methods, since fog is known to produce changes in the potential gradient (PG). Many aspects of the relationship between PG and fog remain unexplored, to which modern instrumentation for continuous monitoring of PG and visibility brings a new perspective. We describe several automatic methods of detecting fog events and apply them to a large dataset to understand the evolution of the PG during fog development. The median PG increase in fog is found to be 58 V/m, which is statistically significant compared with the 17 V/m standard deviation of PG in the prefog hours. However, the median lead time of this increase before the fog onset was found to be 0.4 h, compared with 0.6 h solely using visibility data. While we were able to predict fewer fog events using PG (55% of cases) than visibility (64% of cases), PG was much more likely to give a longer lead time (of over 2 h) than visibility (30% vs. 13% respectively). This indicates that PG measurements would be a useful additional tool in fog prediction.

KEYWORDS

atmospheric electricity, fog, observations

1 | INTRODUCTION

Fog occurs when the atmospheric visibility is reduced below 1000 m as a result of water droplets suspended in the air (AMS, 2012). Fog can cause a significant disruption to transportation.[1] This could be mitigated with accurate forecasts. However, even with modern techniques, it is still very difficult to forecast fog using numerical weather prediction (NWP) methods (Fernando et al., 2021). Consideration of direct observations, such as visibility, has been found to be helpful in predicting fog conditions (Clark et al., 2008). Atmospheric electricity measurements present a possible further source of information, which has hitherto been relatively unexplored. Opportunities for exploiting atmospheric electrical measurements to improve fog prediction are evaluated here using data from many radiation fog events observed on the University of Reading campus in the UK.

There are generally two approaches to short-range forecasting of fog events. One is to use NWP, possibly including assimilation of real-time measurements for NWP-based nowcasting such as in Clark et al. (2008).

These could be parameters commonly used in NWP, such as temperature, or they could require special implementation, such as the potential gradient (PG). The other method is to develop an observation-driven nowcasting system, such as the PARAFOG2 method described in Ribaud et al. (2021), which uses visibility and lidar to predict fog with lead times of around 0–2 h. If the PG can be shown to give predictive information prior to the onset of fog, PG measurements could theoretically be used in either type of system: as a component in NWP-based nowcasting or as a basis for an observation-based nowcasting system that would be used as a complement to other methods.

1.1 | Previous work on fog and atmospheric electricity

As early as the late 1700s, it was observed that fog had an effect on atmospheric electricity (as mentioned by Ronayne, 1772, in a letter to Benjamin Franklin). Chree (1908) further observed that the PG measured at Kew in London was often increased by a factor of several times during fog.

By the 1960s, several authors had begun to investigate whether PG changes could be used to predict fog. Serbu and Trent (1958) found that the air's electrical conductivity began to decrease up to an hour before fog developed, which seemed to suggest a possibility of forecasting. Anderson and Trent (1962) found similar results in a study of fog at sea. In two reports (Dolezalek, 1962, 1963), Dolezalek combined results from a number of investigations and reported that the conductivity would generally change 30–120 minutes before the visibility reduced below 1000 m. Finally, Anderson and Trent (1966) evaluated the usefulness of this phenomenon for fog prediction for several months of data, reporting that they had found PG to be a valuable forecasting tool.

However, not all authors came to the same conclusion. Ottevanger (1972) performed a similar study in the Netherlands and reported that measurements of the conductivity were no more effective for predicting fog than measurements of the visibility, which are simpler and more routinely made. Dolezalek responded to this by noting that the electrical fog prediction method was not meant to be used on its own but rather in conjunction with other fog prediction techniques (Dolezalek, 1973).

Paugam (1978) performed a study on using electrical measurements to predict fog in a variety of conditions, this time using continuous measurements of PG, conductivity, and visibility for around 40 fog cases in Guissény, France. He concluded that this technique was adding nothing beyond that of existing meteorological measurements, stating:

> The analysis of our results shows that during periods of fog, it is generally the case that the simultaneous measurement of electrical and meteorological parameters does not provide much more predictive information than the measurement of the latter alone. *(This author's translation.)*

More recently, Nizamuddin and Ramanadham (1983) looked at electrical measurements in haze and mist as well as fog during a number of case studies, finding that the PG increased during their formation. Deshpande and Kamra (2004) made measurements of the particle size distribution over the sea during fog alongside PG measurements, finding evidence that aerosol and droplets alter electrical conductivity. Anisimov et al. (2005) looked in greater detail at spatial electrodynamic structures in fog. Recently, Yair and Yaniv (2023) have reported on fog PG measurements, finding highly increased PG values during several fog case studies.

In summary, several authors have suggested that the PG could be useful in predicting fog, while others have found this not to be the case. Even though some have stated that electrical measurements are not useful for fog prediction, the inconclusive outcome has sustained interest in this topic. Some of this uncertainty is due to the fact that most studies on fog and atmospheric electricity have focused on a relatively short time frame or a few cases. A long-term study would help us to understand the average behaviour of the PG in fog.

In this work, we will address this question with a much larger fog dataset created using modern, automatically recording instrumentation. At the University of Reading, continuous measurements of the PG alongside daily manual fog measurements and automatic meteorological measurements exist since 2005. Automatic continuous measurements of visibility are available since 2019. This collection gives us high-temporal-resolution measurements (one-second sampling period averaged into five-minute intervals) of the PG in over 100 fog events made over 20 years. Through analysing such a large dataset, we consider the value of using PG measurements to predict fog.

1.2 | The electrical effects of haze and fog

Electric fields exist throughout the atmosphere as a result of the electric potential difference between the conductive upper atmosphere and the Earth, typically 240 kV (Williams, 2009). This potential arises from charge separation in thunderstorms and electrified rain clouds across the globe, and it results in a "fair-weather" electrical

current towards the surface in regions of fair weather. The PG[2] has been monitored at surface stations in various locations for over a century (e.g., see Harrison & Ingram, 2005), and it is useful as a measurement of both global and local atmospheric conditions, since it is affected by both the ionospheric potential (a largely global phenomenon) and air conductivity (which is locally determined).

The classical understanding is that fog affects PG measurements as a result of droplets altering the conductivity of the atmosphere (Bennett & Harrison, 2008). Fog and haze droplets tend to remove small ions (which give the air its conductivity) from the atmosphere. This occurs to some extent during the prefog conditions when small haze droplets exist, as well as during the fog event itself. This removal of ions changes the electrical environment of the air, as described in more detail below.

On short timescales and in conditions when no active charge separation is occurring, the vertical air–Earth current density J_z is relatively constant. Therefore, when the conductivity (σ) changes, the PG (F) changes proportionally according to Ohm's law:

$$F = J_z/\sigma. \tag{1}$$

The atmosphere is electrically conductive due to the presence of mobile cluster ions, which are produced in the air by high-energy particles. Near the surface of the Earth, this is mostly due to a combination of Galactic cosmic rays (GCRs) and radioactive emissions from the decay of terrestrial radon and its daughter products (Harrison et al., 2010). The total conductivity of the air is given by

$$\sigma = 2n\mu e, \tag{2}$$

where n is the mean number concentration of ions for a parcel of air, μ is the mean ion mobility, and e is the elementary charge.

We can estimate the number concentration of ions by solving the ion-balance equation (Harrison et al., 2010) (assuming the monodisperse case, i.e., that all droplets are the same size):

$$\frac{dn}{dt} = q - \alpha n^2 - \beta n Z, \tag{3}$$

where q is the volumetric ion production rate, α is the ion–ion recombination coefficient, β is the ion–droplet attachment rate (which depends on droplet size and concentration), and Z is the droplet concentration. In a polydisperse case, further droplet loss terms can be added to represent a range of sizes.

In the steady state, Equation (4) becomes

$$n = \frac{\sqrt{\beta^2 Z^2 + 4\alpha q} - \beta Z}{2\alpha}. \tag{4}$$

When haze or fog forms, both the droplet concentration and the ion–droplet attachment rate increase considerably, which means that the ion concentration at equilibrium decreases, which then increases the PG according to Ohm's law. The final relation is

$$F = \frac{J_z \alpha}{\mu e\left(\sqrt{\beta^2 Z^2 + 4\alpha q} - \beta Z\right)}, \tag{5}$$

so that in fog or haze the PG depends primarily on the vertical current (J_z) and the droplet size and quantity (βZ), as the other terms vary much less.

In the real world, this simplified theoretical treatment is often complicated by a variety of other simultaneous changes in the atmosphere during fog (e.g., increase in aerosol pollution due to stable boundary layer, changes in ion generation, etc.). Therefore, in order to understand the true behaviour of the PG in fog, it is necessary to characterize measurements in real-world fog cases.

In this article, we will examine a large collection of real-world fog events. In Section 2, we will describe several ways of automatically detecting fog events in a large, high-resolution meteorological dataset. We will present methods to detect fog using measured visibility data, as well as a method based only on other meteorological measurements when visibility is not available. Then, in Section 3, we will apply these methods to analyse many fog events, particularly the behaviour of the PG.

2 | AUTOMATICALLY DETECTING FOG EVENTS

2.1 | Reading University Atmospheric Observatory

In order to capture a wide variety of radiation fog events, we have analysed automatic high-resolution measurements at our university's meteorological observatory in Reading, UK (51.44136°N, 0.93807°W).

The University of Reading began making meteorological measurements in 1901 (Brugge & Burt, 2015), with automatic readings at the current observatory site beginning in 1997 and PG measurements in 2005. The Reading University Atmospheric Observatory (RUAO) is located on the university's Whiteknights campus, and is in a relatively open area surrounded by grass, with some trees, buildings, and a small lake in the wider area.

For this study, several instruments in particular are used, including a Chubb JCI 131 electric field mill for PG (mounted at a height of 3 m), a Biral SWS-250 present weather sensor for visual-range measurements (which we use synonymously with visibility in this article), a

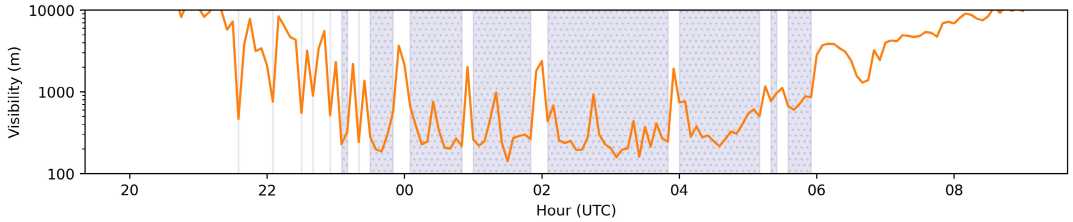

FIGURE 1 Measurements of visibility during a fog event on April 21–22, 2023. The blue filled-in areas indicate periods when the visibility is lower than 1000 m.

Kipp & Zonen CNR4 net radiometer, Campbell Scientific PRT thermometers for dry and wet bulb temperature, a Rotronic HC2-S3 humidity sensor (in a Stevenson screen), and a Vector Instruments A100LM propeller anemometer on a mast at 2 m for wind speed. In this article, we have used five-minute averages from these instruments, derived from one-second samples for most instruments and one-minute samples from the present weather sensor.

2.2 | Methods for detecting fog

Fog is defined by conditions in which the visibility is reduced to below 1000 m. This practical definition is appropriate for many applications, such as aviation, in which the primary need for defining fog is to make pilots aware of atmospheric conditions at a specific time and place. However, for the study of fog prediction, such a simple definition is insufficient for many needs, such as quantifying the lead time of a forecasting technique.

For example, in this study, to investigate the PG during the time leading up to fog events, a definition for a fog "event" is needed, rather than simply an instantaneous diagnostic of fog or no fog.

As seen from an example fog event in Figure 1, the visibility during a single day of radiation fog does not instantly change from above to below 1000 m. Instead, it often enters a period in which there are occasional short episodes of low visibility followed eventually by a longer period of low visibility. Each individual episode of low-visibility measurements should not be seen as an individual fog event. Rather, to a human observer, this would only be classified as a single fog event.

However, it appears that there is no method described in the literature to identify a fog "event" as such. In this article, we develop and describe methods for doing so. In addition, we also explore methods of looking for fog events in meteorological datasets *without* automatic visibility measurements (i.e., using only thermodynamic and similar quantities to infer the presence of fog).

The methods for identifying fog events described in this article are summarized in Table 1. In the following sections, we will describe each method in more detail.

2.3 | Detecting a fog event with visibility

Since fog is defined by visibility, it is possible to use visibility measurements directly to identify events. Two such methods are described below.

2.3.1 | Manual observations and instantaneous visibility

As a reference for comparing other methods, we use observations of fog recorded by expert observers daily at the site at 0900 UTC. This is a simple binary subjective observation of whether fog is present or not, and it is likely to be a robust measure in the vast majority of cases.

We also have used the automatic visibility measurements in a similar manner to compare the Biral SWS-250 visibility with the manual observations, in order to provide a baseline for the automatic measurements. To do so, we simply evaluate whether the visibility is less than 1000 m at 0900 UTC. If it is, then the circumstances can be considered to be those of fog.

2.3.2 | Visibility-timing algorithm

The second method is to use the visibility with a threshold for the minimum length of time for which the visibility can be over and under 1000 m to be considered a single fog event. For example, in this study, we require fog events to last at least an hour, with an allowance of gaps of up to 45 minutes before the event is broken. Since this method may detect two fog events with only a short gap between them, it is also necessary to require a certain length of clear air before the event start. This ensures that the "prefog" development time does not include another fog event.

TABLE 1 Methods for defining a fog event. Visibility uses visual range, measured by an automatic present weather sensor.

Method	Description	Example
Manual observations	Measurements of present weather by human observers	"There was fog today"
Instantaneous visibility	Visibility measured at a single time (such as 0900 UTC)	visibility < 1000 m
Visibility-timing algorithm	Fog event defined based on length of visibility depression, with allowances for set gap lengths and requirements for a set nonfog length beforehand	Visibility must be below 1000 m for 1 h, but gap lengths of at most 45 min are allowed, and the event must be preceded by at least 1 h with no measurements below 1000 m
Visibility-percentage algorithm	Percentage of visibility measurements below 1000 m in 1 h greater than a given threshold	At least 90% of measurements in an hour are below 1000 m
Meteorological	Fog inferred from humidity and other meteorological measurements	Humidity is greater than 95% and wind speed is below 2 m/s

2.3.3 | Visibility-percentage algorithm

The third approach adds to the second approach. However, rather than specifying the lengths of gaps in the events, only the percentage of visibility measurements in a given hour-long window that are below 1000 m is considered. Any percentage lower than a certain threshold will be assumed to be mist or haze. In this case, we found that a threshold of 90% worked well to find fog events that matched up well with human intuition.

2.3.4 | Performance of methods

It is useful to find a quantitative method for comparing the performance of various fog event detection methods. To evaluate this, a confusion matrix is used, showing true positives, false positives, false negatives, and true negatives. The critical success index (CSI) is used as a measure of the overall performance of the method, which is the number of true positives divided by the number of true positives plus false positives plus false negatives. (In other words, the number of true negatives is ignored, as that makes up the vast majority of cases in fog prediction.)

For reference, an initial comparison is made between the manual observers and the automatic measurement of visibility. The automatic measurements found 32 out of 44 true positives, as well as five false positives (CSI: 0.65). This is generally good agreement, although there are some cases in which the two do not produce the same results. In other words, occasionally, the observers report fog while the automatic measurement gives a visibility of greater than 1000 m, and vice versa. However, this instantaneous measurement method adds little value to the manual classification. The purpose for automatic classification is to retrieve information about the timing of the fog event, which this does not do.

The visibility-timing algorithm finds 13 true positives and two false positives (CSI: 0.28), and the visibility-percentage algorithm finds 23 true positives and three false positives (CSI: 0.49).

From these results and CSI scores, it is clear that the visibility-percentage algorithm performs better than the visibility-timing algorithm. Figure 2 presents an example to explain why this is the case.

As can be seen in Figure 2, the two algorithms select very different times for the start and end of the fog event. The visibility itself is particularly variable on this day, making this a rather complicated case, though not extremely unusual. The primary issue with the visibility-timing method becomes apparent here, as it incorrectly detects the end of the fog event as occurring just past 2300 UTC. This is because there is a gap that is slightly longer than allowed before the visibility decreases again after midnight. However, there are still two longer, less patchy periods of low visibility afterwards, occurring at around 0200 and 0700 UTC. These are not counted as events, because they follow on too shortly after the initial fog event, and the "prefog" conditions for those events would also contain another fog event, which would be undesirable for analysis.

The visibility-percentage algorithm, on the other hand, does not require this compromise, as it does not consider the very patchy earlier periods of low visibility to be consistent enough to be part of the event, and instead places the beginning and end of the event closer to the less patchy periods of low visibility in early morning. This results in better performance across a variety of fog days.

In summary, the conventional method to study fog is simply to examine instantaneous visibility measurements. However, this does not allow grouping data into *events* for

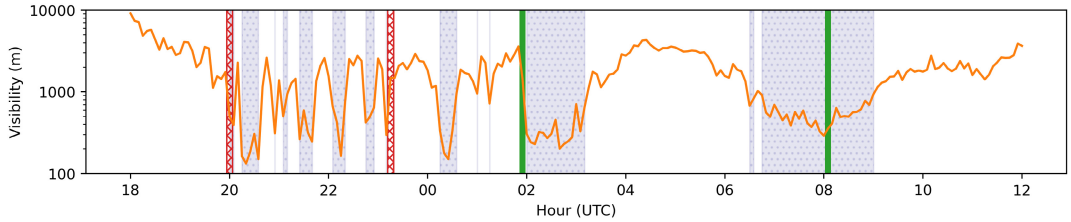

FIGURE 2 Comparison of results of detecting fog events with different methods for an event on January 24–25, 2023. Intervals with visibility less than 1000 m are filled in blue. Start and end times for the visibility-timing event are shown with red hatched bars, and start and end times for the visibility-percentage event are shown with green solid bars. Relative humidity remained above 95% throughout the periods of low visibility.

study of the fog onset. A straightforward means of defining an event is simply to require lengths of time below 1000 m of visibility, but this results in an undesirable trade-off due to the "patchy" nature of many radiation fog events. A visibility-percentage method, based on the number of measurements below 1000 m visibility in a given time period, works much more reliably.

2.4 | Detecting a fog event without visibility measurements

The disadvantage of the above methods is that they require automatic, high-temporal-resolution measurements of visibility, which are a relatively recent addition to measurement sites and are not available in many locations, including our own site before 2019. However, there is a significant amount of meteorological data from decades of measurements that could be used to analyse fog development if fog information could be inferred from them. In some studies, humidity has been used as an indirect measurement of fog. However, this does not often give an accurate estimate, since it is possible to have high humidity without fog. Therefore, we will also evaluate another method that uses thresholds in relative humidity, wind speed, wet-bulb depression, net radiation, and rainfall data to infer the presence of fog. This will be combined with the percentage method for detecting events.

2.4.1 | Choosing thresholds

It is preferable to select the thresholds for the various meteorological parameters mentioned above based on actual fog conditions from measurements. In order to do so, distributions of several variables in fog (90% of measurements in an hour below 1000 m), haze (fewer than 90% but greater than 0% of measurements in an hour below 1000 m), and nonfog conditions (no measurements in an hour below 1000 m) at Reading are plotted in Figure 3.

Several helpful patterns exist in these data. Fog (in Reading) only forms in relatively cool weather when the temperature is below 20 °C, wind speeds are below 2 m/s, and the humidity is high. (The wet-bulb depression provides a helpful second measure of humidity that allows for robust measurements if either RH or wet-bulb depression sensors were to malfunction, for example.)

Specifically, in the net radiation, we note a significant difference between the haze and fog measurements. It appears that the net radiation is most often near zero in fog, while it is mostly negative in haze. This is because the mature fog has become opaque in the portion of the infrared spectrum that is measured (30–50 μm), as its droplets have grown enough to absorb that energy, which changes the net radiation.

For other variables, suitable values are chosen based on the distributions given. From these, we find a new set of thresholds for detecting fog, as shown in Table 2. Temperature did not contribute to improved fog detection, while humidity and net radiation were critical. Note that the time threshold (before noon) was chosen to include only night-time radiation fog, as this performed more consistently than afternoon and evening events.

With the final thresholds, we found that 19 true positives were detected, with 65 false positives and 25 false negatives (CSI: 0.17). While this is nowhere near perfect, the false positives are a vast improvement over just using humidity thresholds (which gave 37 true positives and 160 false positives). In addition, by verifying detected events with human observations at 0900 UTC, we can eliminate the false positives and increase artificially the CSI to 0.43. In other words, the human observations are used to detect the events, but the meteorological method is used to give an estimate on the timing (i.e., start and end time) of the fog event.

2.4.2 | Timing

The purpose of developing these additional methods of fog event detection over simply using manual observations

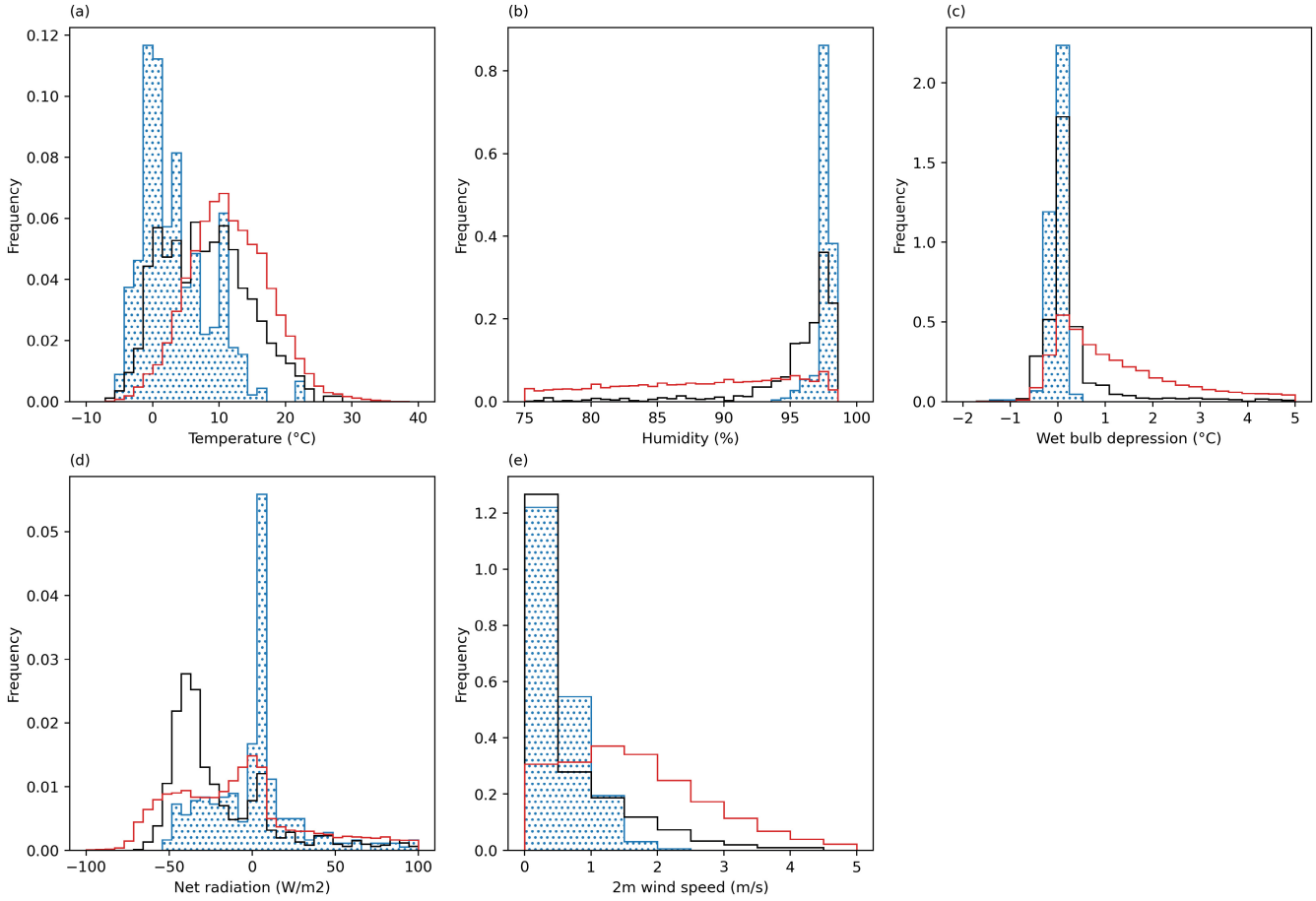

FIGURE 3 Histograms of measurements of (a) temperature, (b) humidity, (c) wet-bulb depression, (d) net radiation, and (e) 2-m wind speed in fog, haze, and nonfog air. The blue hatched area denotes fog conditions, the black line is haze, and the red line is nonfog.

TABLE 2 Thresholds for detecting fog.

Name	Greater/less	Value
Relative humidity	Greater	95%
2-m wind speed	Less	2 m/s
Net radiation	Greater	$-20\,W/m^2$
Net radiation	Less	$30\,W/m^2$
Wet-bulb depression	Less	0.2 °C
Time	Before	1200 UTC

is to provide additional timing information. Therefore, it is desirable to evaluate the accuracy of the timing of this method before using it. To do so, we compare the detected start and end times for each fog event with the corresponding event detected with the visibility-percentage algorithm.

Figure 4b shows a histogram of the time offsets between the meteorological method and the visibility-percentage method. Most cases have a very small offset (examination of individual events confirms this), but there are some events that are offset by a number of hours from the actual event time. This is unfortunate, as it prevents the meteorological method from being used for accurate timing comparisons. It is, however, still performing considerably better than using humidity as a threshold alone, which regularly shows a timing discrepancy of up to half a day, shown in Figure 4a.

Data time series from individual fog events show that morning radiation fog's timing is best predicted by a small jump in the measured net radiation. The transition from "haze" to fog is often marked by a rapid change in net radiation from a negative value to a near-zero value, as the droplets begin to absorb more of the upwelling radiation and reradiate it back to the surface. It was found that an increase above $-20\,W/m^2$ (towards positive values) was generally associated with fog formation. This is the same behaviour of optically "thick" fog as reported by Price (2011). In the evening, the radiation changes were different, and this threshold did not perform as well in detecting the start of fog events. (For this reason, only morning fogs are considered in the meteorological method during this analysis.)

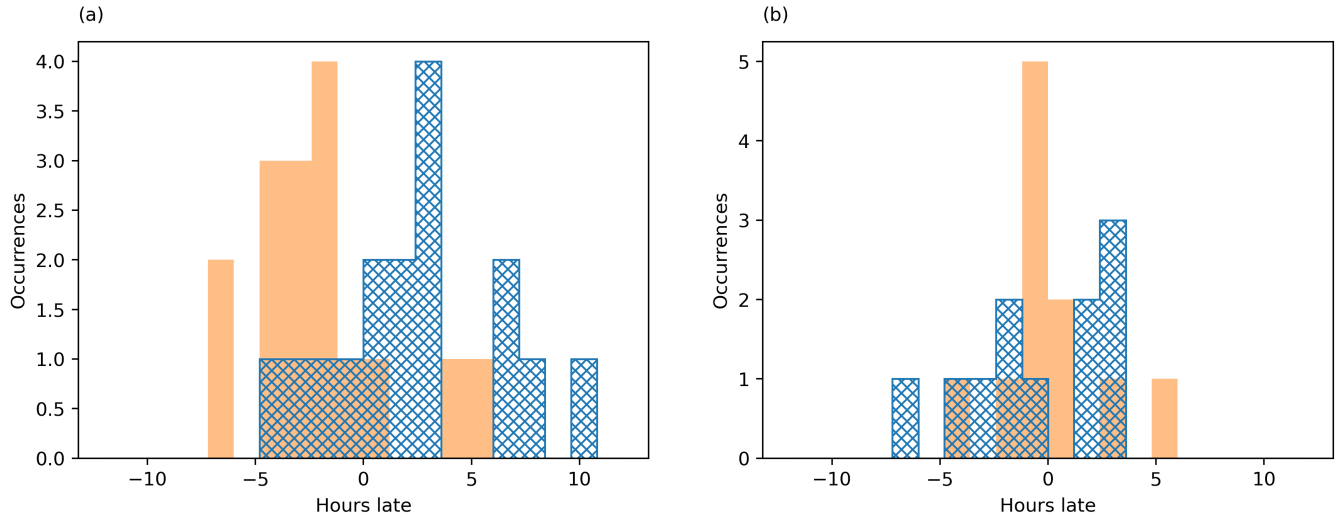

FIGURE 4 Timing of groups detected using (a) a humidity threshold and (b) the meteorological method compared with visibility-percentage algorithm. Start offsets are shown in solid orange and end offsets are shown in hatched blue.

TABLE 3 Evaluation of methods for detecting fog.

Method	Advantages	Disadvantages	Critical success index
Manual observations	Very accurate diagnostic, can be used for verification	Little to no timing information, only available at 0900 UTC	(truth)
Instantaneous visibility	Easily measured and very accurate	No timing information	0.65
Visibility-timing algorithm	Based on accurate measurements, simple concept	Difficulty in fog event detection, only in data after 2019	0.28
Visibility-percentage algorithm	Based on accurate measurements	Only available in data after 2019	0.49
Meteorological	Available for long time series	Slightly lower accuracy at detecting events, poor timing determination	0.17 (0.43 with false positives removed by cross-checking with manual events)

2.5 | Summary of methods

In Table 3, we compare the advantages and disadvantages of using the methods described here to detect fog events. Included in the table are the CSI scores for accuracy of detections compared with the manual observations.

In summary, the manual observations and instantaneous observation methods, which have both been used conventionally, do not provide information on the start and end timing of a fog "event." The visibility-timing algorithm does give this information, but it does not capture real-world fog events accurately due to the often patchy nature of visibility during fog days. The visibility-percentage method works similarly but performs much better. Therefore, this is the method we use throughout the remainder of this article when visibility data are available. When visibility data are not available, we use the meteorological method instead, although that is not as precise in identifying the timing of events.

3 | ANALYSIS OF DETECTED FOG EVENTS

With the methods presented in Section 2, we will investigate fog development and dissipation using measurements made at the University of Reading Atmospheric Observatory. With the visibility-percentage algorithm, we have access to high-quality timing data on over 40 fog events since 2019. In addition, using the meteorological method, we can investigate fog data from events dating back to 2005, when the electric field mill was originally deployed.

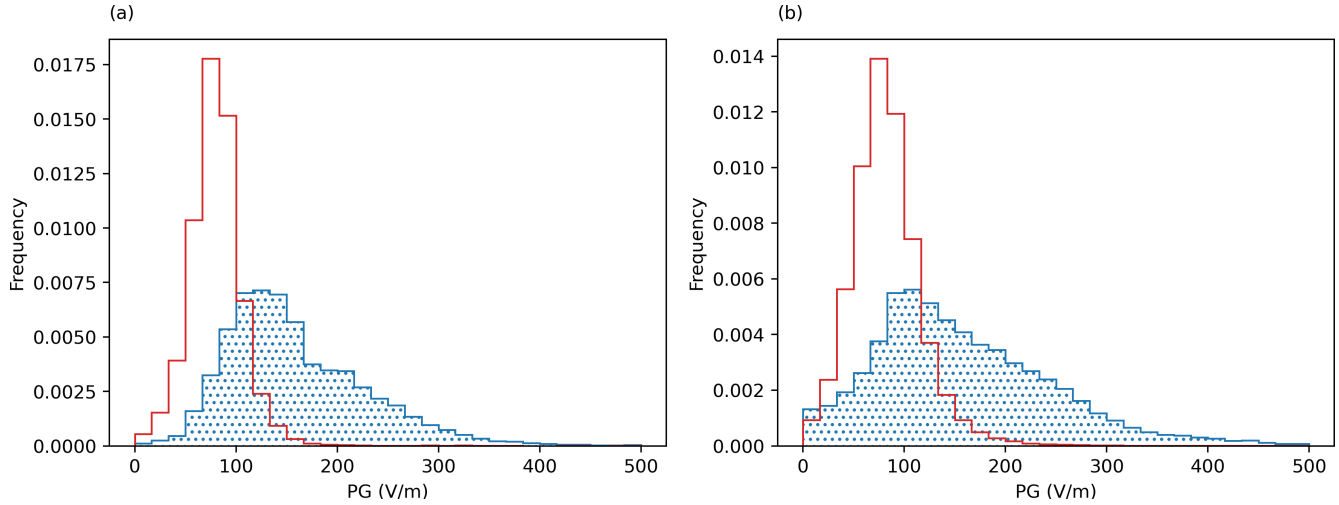

FIGURE 5 Distribution of PG in fog based on (a) the visibility-percentage method and (b) the meteorological method (which includes data back to 2005). Fair-weather data are shown by a red outline, while fog data is shown with blue hatching.

In total, this provides five-minute-resolution data on fog that we can analyse for nearly 20 years of fog events.

As discussed earlier, many decades of occasional studies have still left open the question of the exact behaviour of the PG during fog and fog formation. With a collection of 137 detected fog events (47 with visibility data and 90 without), we are now prepared to look at the PG behaviour in general conditions.

In this article, we have removed the variation due to the typical diurnal cycle from PG values. During a typical day, the PG undergoes a cyclic variation due to factors unrelated to fog, such as changes in global thunderstorm activity in the global atmospheric electric circuit, as well as other local diurnal effects, such as rush-hour pollution (e.g., see figure 10 in Nicoll et al. (2019) for a detailed discussion of the diurnal PG variation at Reading). Therefore, to ensure that measurements of changes in PG during fog (which often occurs at similar times of the day) are due to the fog itself rather than other factors, we have subtracted the mean wintertime variation from the median of the PG for the given time of day from all PG values. The maximum magnitude for this correction is around 35 V/m during the evening (UTC). This should remove the global diurnal cycle. More information on the removal of the diurnal cycle is given in the Supplemental Information.

3.1 | Changes in PG

We begin this analysis with an examination of the distributions of PG measurements during fog.

In Figure 5, we compare the PG during fog with the PG during fair weather. This includes 47 events using the visibility-percentage method and 90 events from the meteorological method, for a total of 137 events. The fair-weather data points are selected according to the fair-weather criteria presented in Harrison and Nicoll (2018), except for the cloud height requirements (which were not available in all measurements). The PG is higher during fog (median 144 V/m for data from the meteorological method and 137 V/m for visibility data from the visibility-percentage method) than it is during fair weather (79 V/m from the meteorological method and 82 V/m from the visibility-percentage method). The medians of each distribution are nearly identical for the two fog identification methods; however, the distributions show less overlap (which indicates different values) in the visibility-percentage method. This is likely due to false positives, in which there are actually some nonfog measurements, shown in Figure 5b, which bring down the overall PG distribution. Nonetheless, from both methods, the median PG during fog is still significantly higher than that during fair weather.

Next, we consider the evolution of the PG throughout fog events by compositing many events relative to the fog event start time. Since the meteorological method is less accurate in detecting the exact start time of the fog, this only considers the visibility-percentage method events.

In Figure 6, the distributions of PG values for each time bin for 47 fog events before and after the fog event start are shown. As we can see in Figure 6a, there is a marked increase in PG in the hours leading up to fog development, leading to a median peak of around 200 V/m an hour after the event start, with a slower decrease in the PG before fog dissipation.

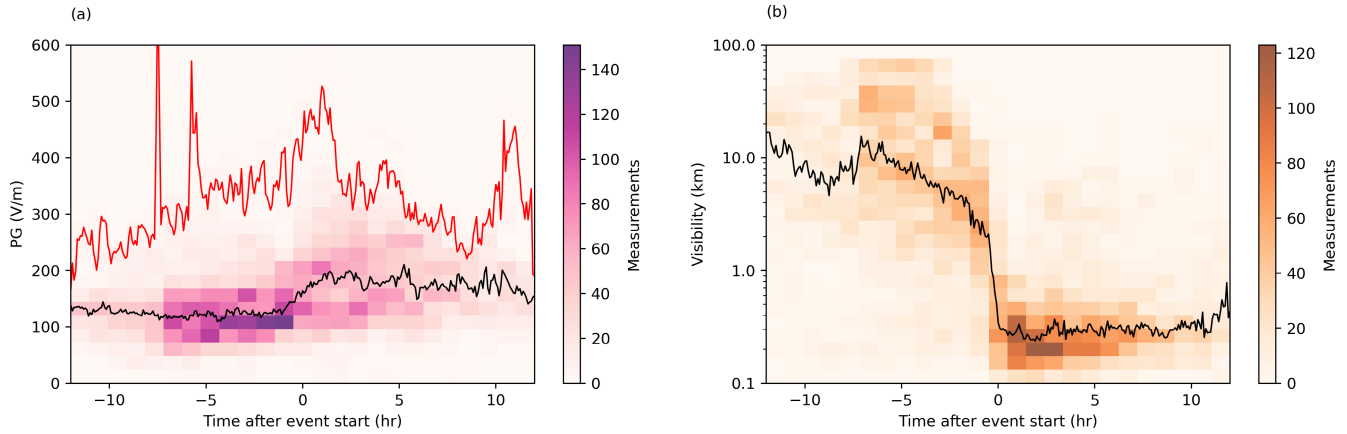

FIGURE 6 Histogram across time of composites of (a) PG and (b) visibility during all fog events, with median (black line) and 99% quantile (red line, PG only). Time zero is the beginning of the fog event, as defined using the visibility-percentage method.

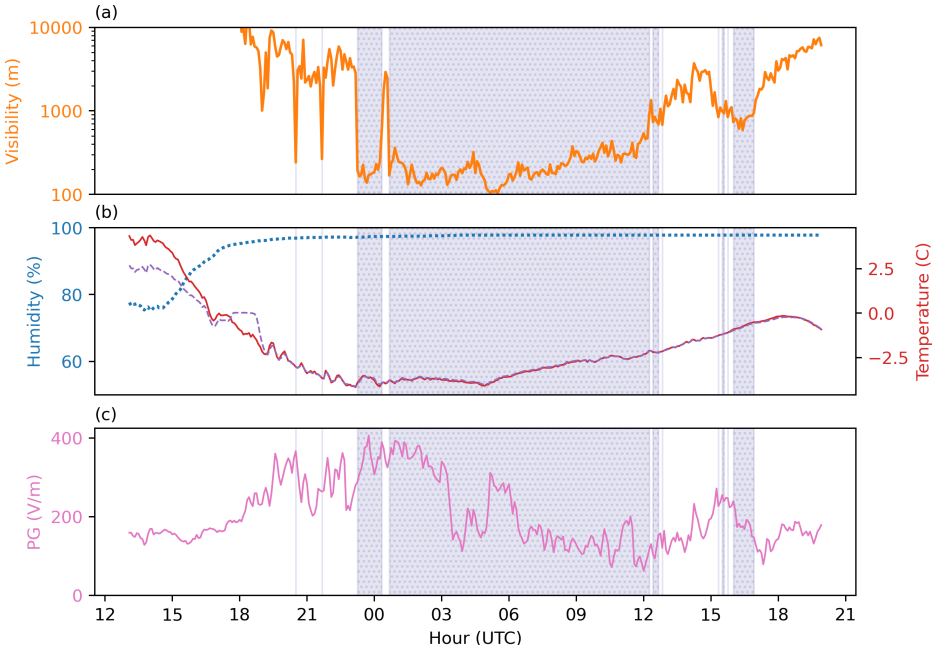

FIGURE 7 A fog event on December 10–11, 2022, with a large PG increase, with several variables plotted. (a) Visibility on a logarithmic scale. (b) Dry (red) and wet-bulb (purple dashed) temperatures, as well as the humidity (blue dotted). (c) PG. Intervals during which the visibility is below 1000 m are shaded blue.

In Figure 6b, we include a similar plot showing the change in visibility. This confirms that we are indeed aligning the events correctly. It also shows that the change in visibility prior to the event start is quite rapid, falling sharply from over 2000 m to under 300 m in the hour before fog onset.

Furthermore, we can see that the median PG begins to rise about 2 h before the event start (this timing is investigated further in Section 3.3). In addition to this, the 99% quantile increases to over 500 V/m in the 6 h before the event begins, indicating that a few events show a large increase even earlier before the detected event start.

From these distributions, it is also apparent that there is much variation in the magnitude of the PG change. We can see this in the two case studies presented below.

In Figure 7, the PG increases to around 400 V/m (much higher than typical fair-weather values) during the main portion of the fog event. This is a good example of a case with a large PG increase. However, in Figure 8 there is no such increase, with PG values within the normal fair-weather range throughout the entire event. The difference between events such as these, as well as many other events that are often somewhere between these two, is not clearly apparent (although the temperature in Figure 7 is lower than in Figure 8).

We can better quantify the number of events that show measurable changes in the PG by plotting a distribution.

Figure 9 shows the changes in PG during each fog event detected by the visibility-percentage method, calculated by taking the mean PG value during the first 2 h of the fog

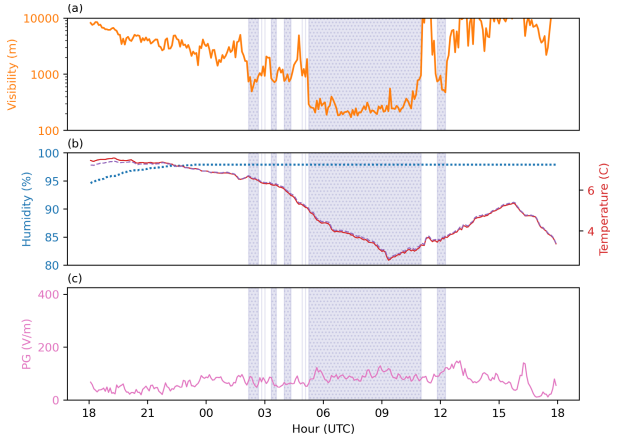

FIGURE 8 A fog event on December 18–19, 2021, without a large PG increase, with several variables plotted. (a) Visibility on a logarithmic scale. (b) Dry (red) and wet-bulb (purple dashed) temperatures, as well as the humidity (blue dotted). (c) PG. Intervals during which the visibility is below 1000 m are shaded blue.

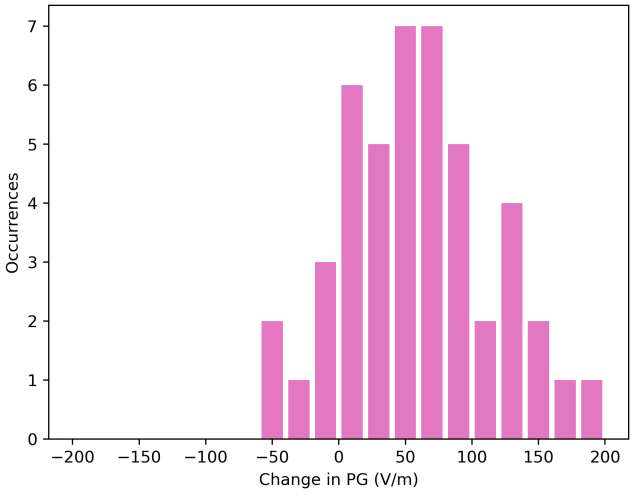

FIGURE 9 Histogram of changes in PG between the mean PG during the first 2 h of fog and the mean PG during the period from 3 to 6 h before fog start.

event and subtracting the mean PG that was measured from 3 to 6 h before the fog started. In this way, we consider the short-term change, rather than magnitude, of the PG. From this plot, we can see that the majority of cases do indeed see an increase, with a median of 57.6 V/m. However, the PG *does not always* increase during the 3 h leading up to fog. It does increase in the majority of events, but in six out of 47 cases (13%) shown here there is a small decrease. Further study is needed to understand why fog does not result in an increased PG in these cases. (Fog droplet collection is not the only phenomenon that affects the PG during a real-world fog event.)

3.2 | Variability in PG

We are also able to quantify the change in variability of the PG during a fog event. It is simple to do so using the standard deviation over a moving time window. However, we do not want to define a time window arbitrarily (of say, 20 minutes) and miss an important change in variability at some other timescale. Therefore, we create a two-dimensional plot of the standard deviation during the onset of fog (averaged for all visibility-percentage events) with an axis for time window, as shown in Figure 10a.

From Figure 10a there is an obvious increase in the variability of the PG during fog, beginning shortly before the fog events start. The areas with higher standard deviations in this plot show us the timescales at which PG changes during fog. In this case, the increase seems to be largest on scales of over three quarters of an hour, which suggests that most of the PG changes captured in this data are longer-term, rather than rapid changes. This increased variability appears to be mostly due to the larger-scale changes in PG associated with formation of fog. (Note that small-scale variation associated with turbulence would not be captured by five-minute data, so such variation may exist as well but would not be visible in this plot.) It is also key to note that the variability remains high or even increases in the hours after the fog forms, suggesting that the PG continues to change after the fog has formed. This is consistent with PG measurements from individual fog events such as in Figure 7, in which there are large changes in PG during the event even as the visibility remains relatively constant and low.

A similar plot, but for logarithmic visibility, is shown in Figure 10b. The major difference is that visibility becomes more variable prior to the onset of fog (and for smaller timescales) but is much less variable during the fog itself. The variation in visibility is largest for longer timescales near the start of the event, which is consistent with the definition of an event based on visibility.

3.3 | Timing of PG changes

It was shown in Section 3.1 that the PG does indeed increase during fog events. However, in order for this to be used as a prediction tool, the increase must be identified to occur *before* the fog itself is already developed. Otherwise, it only provides a diagnostic for fog, which is already known. To quantify whether this is the case, we can study the lead time of the change in PG above typical prefog values.

We assume that the PG becomes "predictable" not when it begins to rise but when it increases and exceeds the typical variation expected during prefoggy conditions.

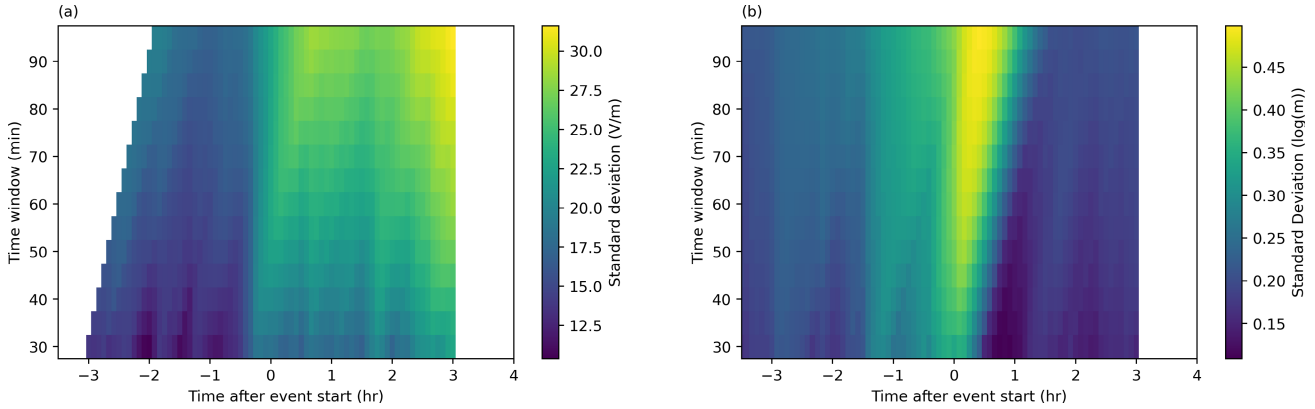

FIGURE 10 Plot showing the standard deviation for various timescales before and after fog event start. (a) Standard deviation in PG and (b) log10 visibility.

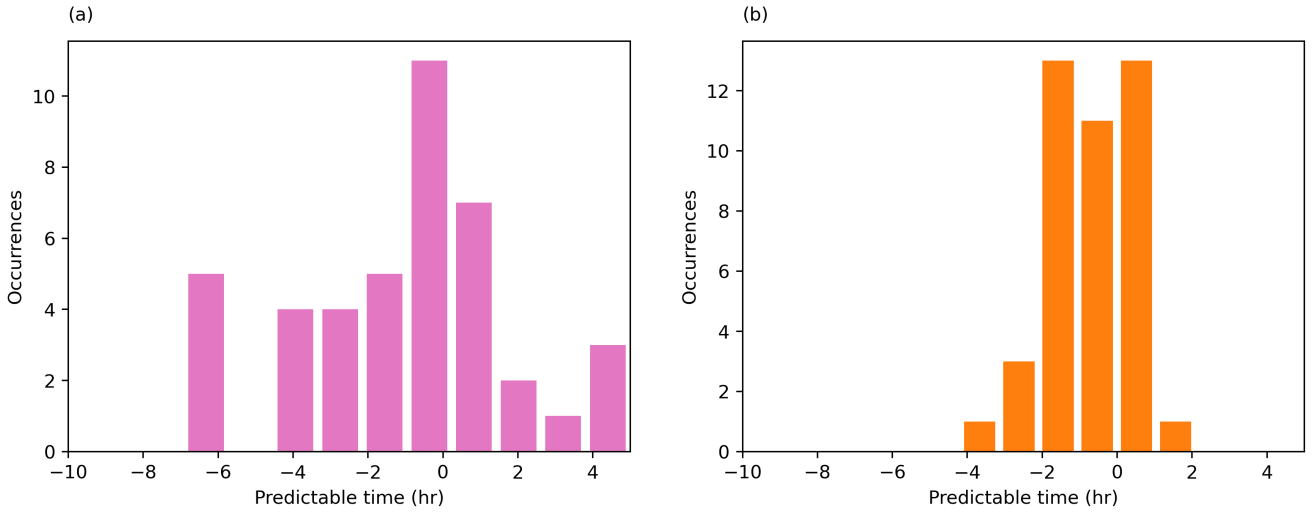

FIGURE 11 Histogram of advance timing for two-standard-deviation change from the 3–6 h mean value before fog start, for (a) PG and (b) visibility.

We already have an estimate of that variability from Figure 10a: 17 V/m. A histogram is plotted showing the lead time before the diagnosed fog event start time for each event when the PG first increased above its hourly mean by at least twice the standard deviation of 17 V/m, which could have hypothetically been interpreted as a sign that fog would form. This is shown in Figure 11a.

In 55% of the events, PG increased by the required amount before the fog event started. Thus, for almost half of the events, even though the PG increased to a higher value during the fog event, it did not do so early enough for the event to have been predicted based on PG. The mean lead time for this increase was 0.4 h. However, 30% of the events had lead times of greater than 2 h. In addition, 9% of the events did not increase above the typical variation.

We can compare this with visibility measurements (on a logarithmic scale), since visibility is more closely tied to the phenomenon of fog, and such sensors are much more widely deployed than field mills. A similar plot, but with visibility, is shown in Figure 11b. Here, a typical prefog standard variation of 0.3 log10(metres) is used (again doubled), based on the same reasoning as used for PG. This method sees a general improvement from using PG. In this plot, 64% of the events decreased below that threshold before the event start, and the median lead time was 0.6 h, while only three events did not decrease below the threshold, but only 13% of the events had lead times greater than 2 h.

4 | DISCUSSION AND CONCLUSIONS

In this article, we have examined the behaviour of the PG during fog, after removing diurnal variations that are not associated with fog. This topic has been studied for

many years, and results have not been consistent across various studies. Studies of shorter timescales, such as Serbu and Trent (1958), Ottevanger (1972), and Yair and Yaniv (2023), have shown conflicting results. Therefore, we have developed several methods for categorizing fog events in long datasets automatically, which allows us to study the behaviour of the PG during many fog events. This novel technique of fog event start detection makes it possible to compare the development of many fog cases side-by-side.

We have found that our most accurate fog event detection method is the visibility-percentage algorithm, although we continue to use the meteorological method alongside manual observations, when visibility measurements are not available, since this still provides valuable additional data. The timing using the meteorological method, while still not entirely precise, was greatly improved by using net radiation to identify fog onset.

Based on the analysis of these events, it has become clear that the PG at Reading does generally increase during fog, with a median change of 58 V/m. While this is a small change, it is statistically significant, given that the typical standard deviation in prefog conditions is around 17 V/m. Further, this study finds that the PG changes enough to have predictive value before the fog event less often than the visibility (55% vs. 64% of cases, respectively), and the median lead time is shorter (0.4 vs. 0.6 h). However, PG is much *more* likely to have a long lead time of over 2 h, with 30% of fog events showing this increase, compared with only 13% showing long lead times for visibility.

This clarifies the apparent contradiction between various authors' results in the previous literature. Indeed, these data do confirm that, in some cases, the PG is no more useful for predicting fog than visibility measurements alone. However, it is also clear that there are many fog events that do in fact show a significant increase hours in advance of the visibility change, confirming the results of other authors. Therefore, it appears that there is valuable predictive information available in PG measurements beyond that solely available from visibility data, even though this pattern does not occur in all fog events.

The results of this study apply only to radiation fog, as this is almost exclusively the type of fog that occurs at the site in Reading. Radiation fog is important for many applications of this work. However, some of the earlier work on fog and atmospheric electricity, including Serbu and Trent (1958), was done at sea or on the coast, and results may differ from ours, since they measured mostly advection fog. Therefore, additional experiments like this one but in an area with common advection fog may be valuable. Fog event detection methods may also need some adjustment for different locations or fog types. For example, patchiness in visibility during events may differ between sites. Thresholds for the meteorological method may also need to be adjusted for additional fog sites. For example, our wind-speed threshold of less than 2 m/s would likely be unhelpful at a coastal site with advection fog.

These results, showing possible lead times of over 2 h, suggest that PG could be readily implemented into an observation-driven fog nowcasting system. On the other hand, exploiting PG measurements in NWP-based nowcasting (which uses observations to constrain the state of the atmosphere) would require a forward model for changes in PG during haze and fog development, which the assimilation system can compare with observed data. Similarly to Clark et al., 2008, one could conceive of a scheme where prognostic aerosol and cloud water content variables are used to predict changes in PG during haze and fog formation, which could be compared with observations. We are in the process of making continuous measurements of fog and aerosol properties simultaneously with PG and visibility, which could guide the development of such a scheme.

AUTHOR CONTRIBUTIONS

Caleb Miller: data curation; formal analysis; investigation; methodology; software; visualization; writing – original draft; writing – review and editing. **Keri Nicoll:** conceptualization; funding acquisition; methodology; project administration; supervision; writing – review and editing. **Chris Westbrook:** conceptualization; methodology; project administration; supervision; writing – review and editing. **R. Giles Harrison:** conceptualization; data curation; methodology; project administration; supervision; writing – review and editing.

ACKNOWLEDGEMENTS

The authors acknowledge the work of many observers who have collected data and departmental technical staff who have maintained instrumentation at the RUAO site. Caleb Miller acknowledges funding from the National Environment Research Council (NE/S007261/1).

DATA AVAILABILITY STATEMENT

Data from the Reading University Atmospheric Observatory from 1997 to 2023 can be found at the University of Reading Research Data Archive. Miller and Harrison (2023): Measurements from the Reading University Atmospheric Observatory, 1997-2023. University of Reading. Dataset. http://dx.doi.org/10.17864/1947.000490.

ENDNOTES

[1]See, for example, https://www.bbc.com/news/uk-64370940.

[2]The potential gradient, $F = -E = \nabla V$, is the negative of the electric field.

ORCID

Caleb Miller https://orcid.org/0000-0002-1761-8718
Keri A. Nicoll https://orcid.org/0000-0001-5580-6325
Chris Westbrook https://orcid.org/0000-0002-2889-8815
R. Giles Harrison https://orcid.org/0000-0003-0693-347X

REFERENCES

AMS. (2012) Fog. In: *AMS glossary of meteorology*. Boston, MA: American Meteorological Society. Available from: https://glossary.ametsoc.org/wiki/Fog

Anderson, R.V. & Trent, E.M. (1962) *Atmospheric Electricity Measurements In The North Atlantic During Fallex-60*. Interim rept. AD0285573. Washington, DC: Naval Research Lab Washington DC, p. 12 Available from: https://apps.dtic.mil/sti/tr/pdf/AD0285573.pdf

Anderson, R.V. & Trent, E.M. (1966) *Evaluation of the use of atmospheric-electricity recordings in fog forecasting*. AD0643363. Washington, DC: Naval Research Lab Washington DC, p. 22 Available from: https://apps.dtic.mil/sti/trecms/pdf/AD0643363.pdf

Anisimov, S.V., Mareev, E.A., Shikhova, N.M., Sorokinb, A.E. & Dmitriev, E.M. (2005) On the electro–dynamical characteristics of the fog. *Atmospheric Research*, 76(1), 16–28. Available from: https://doi.org/10.1016/j.atmosres.2004.11.026

Bennett, A.J. & Harrison, R.G. (2008) Variability in surface atmospheric electric field measurements. *Journal of Physics: Conference Series*, 142, 012046. Available from: https://doi.org/10.1088/1742-6596/142/1/012046

Brugge, R. & Burt, S. (2015) *One Hundred Years of Reading Weather*. Maidenhead, UK: Climatological Observers Link.

Chree, C. (1908) Atmospheric electricity and fog. *Nature*, 77(1998), 343. Available from: https://doi.org/10.1038/077343b0

Clark, P.A., Harcourt, S.A., Macpherson, B., Mathison, C.T., Cusack, S. & Naylor, M. (2008) Prediction of visibility and aerosol within the operational met office unified model. I: Model formulation and variational assimilation. *Quarterly Journal of the Royal Meteorological Society*, 134(636), 1801–1816. Available from: https://doi.org/10.1002/qj.318

Deshpande, C.G. & Kamra, A.K. (2004) The atmospheric electric conductivity and aerosol measurements during fog over the Indian ocean. *Atmospheric Research*, 70(2), 77–87. Available from: https://doi.org/10.1016/j.atmosres.2004.01.001

Dolezalek, H. (1962) *Atmospheric electric parameter study survey on an effect relating atmospheric electric variations with formation and dissipation of fog*. Wilmington, MA: AVCO Corp Wilmington Mass Research and Advanced Development DIV, AD0284476 Available from: https://apps.dtic.mil/sti/trecms/pdf/AD0284476.pdf

Dolezalek, H. (1963) The atmospheric electric fog effect. *Reviews of Geophysics*, 1(2), 231. Available from: https://doi.org/10.1029/RG001i002p00231

Dolezalek, H. (1973) On the electro-atmospheric fog effect. *Pure and Applied Geophysics PAGEOPH*, 105(1), 907–909. Available from: https://doi.org/10.1007/BF00875840

Fernando, H.J.S., Gultepe, I., Dorman, C., Pardyjak, E., Wang, Q., Hoch, S.W. et al. (2021) C-FOG: Life of coastal fog. *Bulletin of the American Meteorological Society*, 102(2), E244–E272. Available from: https://doi.org/10.1175/BAMS-D-19-0070.1

Harrison, R.G., Aplin, K.L. & Rycroft, M.J. (2010) Atmospheric electricity coupling between earthquake regions and the ionosphere. *Journal of Atmospheric and Solar-Terrestrial Physics*, 72(5), 376–381. Available from: https://doi.org/10.1016/j.jastp.2009.12.004

Harrison, R.G. & Ingram, W.J. (2005) Air–earth current measurements at kew, london, 1909–1979. *Atmospheric Research*, 76(1), 49–64. Available from: https://doi.org/10.1016/j.atmosres.2004.11.022

Harrison, R.G. & Nicoll, K.A. (2018) Fair weather criteria for atmospheric electricity measurements. *Journal of Atmospheric and Solar-Terrestrial Physics*, 179, 239–250. Available from: https://doi.org/10.1016/j.jastp.2018.07.008

Nicoll, K.A., Harrison, R.G., Barta, V., Bor, J., Brugge, R., Chillingarian, A. et al. (2019) A global atmospheric electricity monitoring network for climate and geophysical research. *Journal of Atmospheric and Solar-Terrestrial Physics*, 184, 18–29. Available from: https://doi.org/10.1016/j.jastp.2019.01.003

Nizamuddin, S. & Ramanadham, R. (1983) The electric potential gradient in mist, haze, and fog. *Pure and Applied Geophysics PAGEOPH*, 121(2), 353–359. Available from: https://doi.org/10.1007/BF02590144

Ottevanger, W.P.A.G. (1972) The atmospheric electric fog effect at de bilt. *Pure and Applied Geophysics PAGEOPH*, 95(1), 221–225. Available from: https://doi.org/10.1007/BF00878868

Paugam, J.-Y. (1978) A study of the main atmospheric electric parameters at a little polluted seashore site. PhD thesis Available from: https://inis.iaea.org/collection/NCLCollectionStore/&uscore;Public/45/061/45061311.pdf?r=1

Price, J. (2011) Radiation fog. Part i: Observations of stability and drop size distributions. *Boundary-Layer Meteorology*, 139(2), 167–191. Available from: https://doi.org/10.1007/s10546-010-9580-2

Ribaud, J.-F., Haeffelin, M., Dupont, J.-C., Drouin, M.-A., Toledo, F. & Kotthaus, S. (2021) PARAFOG v2.0: A near-real-time decision tool to support nowcasting fog formation events at local scales. *Atmospheric Measurement Techniques*, 14(12), 7893–7907. Available from: https://doi.org/10.5194/amt-14-7893-2021

Ronayne, T. (1772) XVIII. A letter from Thomas romaine, Esq; to Benjamin Franklin, LL. D. F. R. S. inclosing an account of some observations on atmospherical electricity; in regard of fogs, mists &c. with some remarks; communicated by Mr. William Henley. *Philosophical Transactions of the Royal Society of London*, 62, 137–146. Available from: https://doi.org/10.1098/rstl.1772.0020

Serbu, G.P. & Trent, E.M. (1958) A study of the use of atmospheric-electric measurements in fog forecasting. *Transactions of the American Geophysical Union*, 39(6), 1034. Available from: https://doi.org/10.1029/TR039i006p01034.

Williams, E.R. (2009) The global electrical circuit: A review. *Atmospheric Research*, 91(2), 140–152. Available from: https://doi.org/10.1016/j.atmosres.2008.05.018

Yair, Y. & Yaniv, R. (2023) The effects of fog on the atmospheric electrical field close to the surface. *Atmosphere*, 14(3), 549. Available from: https://doi.org/10.3390/atmos14030549

SUPPORTING INFORMATION

Additional supporting information can be found online in the Supporting Information section at the end of this article.

How to cite this article: Miller, C., Nicoll, K.A., Westbrook, C. & Harrison, R.G. (2024) Evaluating atmospheric electricity changes as an indicator of fog formation. *Quarterly Journal of the Royal Meteorological Society*, 150(761), 1892–1906. Available from: https://doi.org/10.1002/qj.4680